Available online at www.sciencedirect.com
SCIENCE DIRECT
Journal of Colloid and Interface Science 292 (2005) 160–170
JOURNAL OF Colloid and Interface Science
www.elsevier.com/locate/jcis

Studies of the surface charge of amorphous aluminosilicates using surface complexation models

Alejandra A. Jara [a,*], Sabine Goldberg [b], M.L. Mora [a]

[a] *Departamento de Ciencias Químicas, Universidad de la Frontera, Casilla 54-D, Temuco, Chile*
[b] *United States Department of Agriculture, Agricultural Research Service, George E. Brown Jr. Salinity Laboratory, 450 W Big Springs Road, Riverside, CA 92507, USA*

Received 6 January 2005; accepted 19 May 2005
Available online 26 July 2005

Abstract

Synthetic noncrystalline aluminosilicates with variable charge, similar to allophanes present naturally in volcanic soils, were studied. The surface charge behavior was determined by zero point charge (ZPC) measured by electrophoretic mobility (isoelectric points, IEP) and determined by potentiometric titration (point of zero salt effect, PZSE). The ZPC calculated by Parks model (ZPC_c), compared with IEP values, showed that the aluminosilicate (AlSi) surface was slightly enriched by AlOH (34% Al_2O_3 and 66% SiO_2) compared with the bulk composition (29% Al_2O_3 and 71% SiO_2). For aluminosilicate coated with iron oxide (AlSiFe) the ZPC_c (4.4) was lower than the IEP (8.46), showing that the surface composition is formed mainly from iron oxide. The PZSE values for AlSi and AlSiFe were 6.2 and 4.8, respectively. The differences between the IEP and PZSE are attributed to the formation of Si–O–Fe or Si–O–Al bonds; therefore, the reactivity of Fe and Al atoms was modified on the surface. Two mechanistic models, the constant capacitance model (CCM) and the triple layer model (TLM), using the program FITEQL 3.2 were able to describe the surface behavior of both synthetic aluminosilicates. The acidity constants determined using both models for the aluminosilicates showed differences with respect to pure oxide, mainly attributed to the presence of SiOH sites on the internal surfaces. The ionic strength showed a good relation with the parameters obtained using the CCM ($pK^{int}_{a_1}$, $pK^{int}_{a_2}$ and capacitance values) and the TLM ($pK^{int}_{a_1}$, $pK^{int}_{a_2}$, $pK^{int}_{Cl^-}$, $pK^{int}_{K^+}$, and inner capacitance) for both aluminosilicates. However, the TLM was able to describe the acidity and complexation constants better since it considered the formation of the outer sphere complex between the background electrolyte and the surface. Then, the TLM makes it possible to describe real systems.
© 2005 Elsevier Inc. All rights reserved.

Keywords: Amorphous aluminosilicates; Surface charge; Zero point charge; Point of zero salt effect; Isoelectric point; Mechanistic models

1. Introduction

Noncrystalline aluminosilicate compounds and Fe oxide phases in soils are important constituents for many soil reactions because of their large surface area and high chemical reactivity, despite being present in relatively small amounts compared to other colloidal constituents [1–3].

Allophane is an important clay-size aluminosilicate mineral, which occurs widely in andisols [4], a soil typical of southern Chile [5]. It has a spheroidal surface morphology (3.5–5.0 nm) and forms regular aggregates, but its exact structure has not been determined. It has short to mid-range atomic ordering, consisting of Si–O–Al bonding [4].

Allophanes contain mainly alumina, silica, and water in variable proportions and has a typical composition of approximately $Al_2Si_2O_5{\cdot}nH_2O$ [4]. Wada [6] reported some degree of variability in the Si:Al ratio from about 1:1 to 2:1. Because of the small particle size of allophane and its intimate association with other clays (such as smectites, imogolite, or noncrystalline Fe and Al [hydr]oxides and silica), it has proven very difficult to accurately determine the chemical composition of allophane. Consequently, there is always

* Corresponding author. Fax: +56 45 505053.
E-mail address: aljara@ufro.cl (A.A. Jara).

0021-9797/$ – see front matter © 2005 Elsevier Inc. All rights reserved.
doi:10.1016/j.jcis.2005.05.083

some potential error associated with the compositional ratios reported in the literature.

Allophane composition differs depending on the environment in which it is formed. For example, in Si-rich volcanic deposits, the Al:Si ratio of allophane can be as low as 1:1 [2]. The Al and Si chemical coordination in allophanes generate quite different surface charges [7], and therefore the surface enrichment will depend on the surface coordination of these ions (tetrahedron coordination for Si and octahedron for Al). This aluminosilicate mineral has high capacities for specific and nonspecific adsorption of anions, high cation exchange, and water adsorption. The surface area of allophane calculated by crystallography is often found to be about 1000 $m^2\,g^{-1}$, while values measured with ethylene glycol monoethyl ether are in the range of 700–900 $m^2\,g^{-1}$ [6]. The chemical properties of the sites that are dominated by the allophane mineral are largely controlled by the charge characteristics of this mineral component. Due to the complexity of extracting and isolating allophanes of low crystallinity from soils, it is important to obtain synthetic aluminosilicates with properties similar to the natural ones. A number of works have been completed on synthetic Fe and Al oxides that aim to better comprehend the surface reactivity of the natural compounds. Studies by Sposito [8] indicate that the reactivity of the hydroxyl group depends on the metal to which it is attached and the structural orientation of the hydroxides.

Amorphous iron oxides (hydrous ferric oxide and ferrihydrite) are other important mineral constituents of andisols. These compounds have received considerable attention because of their colloidal amorphous structure, determined by X-ray diffractometry [9] and adsorption capacity [10]. The approximate composition of ferrihydrite is $5Fe_2O_3{\cdot}9H_2O$ and it presents a spheroidal surface morphology between 2 and 8 nm in diameter. The surface area of ferrihydrite ranges from 200 to 800 $m^2\,g^{-1}$ and it is a strong adsorbent of phosphate, silica, organic molecules, and heavy metals [10–12].

The study of surface properties of aluminosilicates using surface complexation models (SCMs), such as the constant capacitance model [13] and the triple layer model [14–16], allows us to interpret and to understand the surface charge changes caused by the presence of different types of surface hydroxyl: FeOH, SiOH, and AlOH.

The SCMs employ an equilibrium approach to describe the formation of complexes at an oxide–solution interface and are often used to predict the charge characteristics and ion retention behavior of clay minerals. Charge may arise from chemical reactions at the surface; many solid surfaces contain ionizable functional groups such as –OH (into $–O^-$ and $–OH_2^+$). The electric charge distribution of a hydrous oxide can be explained by the acid–base behavior of the surface hydroxyl group. The charge on these particles is dependent on the degree of ionization (proton transfer) and consequently on the pH of the medium. Most oxides and hydroxides exhibit amphoteric behavior, the charge being net positive at low pH values and net negative at high pH values. At some intermediate pH the net surface charge is zero [17].

These two models consider the surface charge resulting from the dissociation reactions of the surface functional groups (i.e., $–OH_2^+$, –OH, and $–O^-$) and also from the surface complexation reactions. The sign and the magnitude of the surface charge depend on the pH and the ionic strength of the background electrolyte solution. The models are molecular representations of the process of ionic distribution at the solid–solution interface. The purpose of molecular theory is to derive thermodynamic properties such as activity coefficients and equilibrium constants starting from the principles of statistical mechanics.

The aims of this study were (i) to compare the synthetic aluminosilicates with the natural allophanes, (ii) to evaluate the surface composition using isoelectric points and the zero point charges, and (iii) to evaluate the ability of the constant capacitance model and the triple layer model to describe the surface properties.

2. Materials and methods

2.1. Synthesis of the aluminosilicate compounds

Aluminosilicate compounds were prepared using the methodology proposed by Diaz et al. [18] and Mora et al. [19]. First, a co-precipitated aluminosilicate (AlSi) was synthesized. A quantity of 135 mmol of SiO_2 was added as potassium silicate solution to a Teflon beaker containing an $AlCl_3$ solution, the equivalent of 45 mmol of Al_2O_3, at a rate of 0.2 $ml\,min^{-1}$ with continuous stirring, until it reached a constant pH 5.0 (by simultaneous addition of 5 M HCl, dropwise), and was completed with distilled water to a final volume of 330 ml. Finally, the aluminosilicate precipitate was washed repeatedly until no chloride was detected in the supernatant solution.

One part of the AlSi in suspension was coated with iron oxide; Fe^{3+} was added as $Fe(NO_3)_3$ in situ on the AlSi, maintaining the pH (3.0) and temperature (25 °C) constant. Finally, aluminosilicate coated with iron oxide (AlSiFe) in suspension was obtained.

Both aluminosilicates were characterized by their chemical composition, structure, and superficial charge.

2.2. Physicochemical characterization of synthetic aluminosilicate compounds

2.2.1. Chemical analysis

The compositions of the two aluminosilicate compounds were determined by the Bernas method [20]. A 200-mg sample was put in a Teflon Parr bomb, and 1 ml of aqua regia (3:1 HCl:HNO_3) and 6 ml of 48% HF were added. This was allowed to stand for 2 h at 105 °C. After the elapsed time, the solution was transferred to a plastic beaker, 5.5 g

of boric acid was added, and the solution was heated gently until it dissolved completely. The solution was brought up to 100 ml, and the concentrations of Al, Si, and Fe were determined by atomic absorption spectrometry.

2.2.2. FTIR spectroscopy

FTIR spectra were obtained with a Tensor 27 Brucker spectrometer for both aluminosilicate compounds by pressing a 3-mg dry sample into a spectral grade KBr matrix. The resolution of each spectrum was 2 cm^{-1}, scanned 32 times.

2.2.3. The transmission electron micrograph (TEM)

The TEMs were obtained using a Philips Model EM-300 microscope. Each aluminosilicate sample in suspension was dispersed by ultrasonics and one drop of the solution was deposited on a Cu surface, previously covered with a C surface. Finally, the TEMs of the dry sample were recorded.

2.2.4. Mössbauer spectroscopy

^{57}Fe Mössbauer spectra were obtained at room temperature for the samples coated with iron oxides using a constant acceleration Mössbauer spectrometer with a ^{57}Co-in-Pd source. The spectra were plotted with the center of the room temperature iron metal spectrum as the zero of the velocity axis. Spectra were fitted by computer using an iterative procedure assuming a Lorenzian lineshape for each component [21].

2.2.5. X-ray diffraction (XRD)

The samples were scanned from 2° to 30° 2θ using a step size of 0.05° 2θ and scanning for 10 s at each step. The X-ray patterns were collected using Cu$K\alpha$ radiation from a Scintag XGEN 4000 diffractometer generator and a Theta/Theta goniometer equipped with a 1.5° divergence slit, a 0.2° receiving slit, a graphite diffracted-beam monochromator, and a scintillation counter.

2.2.6. Thermogravimetric analysis (TGA)

Approximately 10 mg of dry sample was placed in a platinum pan and heated from 50 to 800 °C (TGA 2950, TA Instruments) using the dynamic-rate high-resolution mode (Res. 5).

2.2.7. Surface area

The total specific surface area was determined gravimetrically for both aluminosilicates (AlSi and AlSiFe) using the retention method of ethylene glycol monoethylether (EGME), as described by Heilman et al. [22].

2.3. Surface charge determination

2.3.1. Point of zero salt effect (PZSE)

The surface charge characteristics of the aluminosilicate samples were measured by potentiometric titration. Aluminosilicate suspensions were prepared by mixing 300 mg of solid samples with 100 ml of KCl at different ionic strengths (10^{-1}, 10^{-2}, or 10^{-3} M). The titrations were done in an N_2 atmosphere at a constant temperature of 25 °C. The titration was initiated from their original pH and 0.2 ml of 0.1 M KOH or HCl was added every 20 min. The pH response of the electrode was calibrated with buffer solutions at pH 4.00, 7.00, and 10.00. The point of zero salt effect (PZSE) was determined by locating the common point of intersection of the potentiometric titration curves at different ionic strengths.

2.3.2. Isoelectric point (IEP)

The samples were suspended in KCl (10^{-3} M) and electrophoretic mobility measurements were performed in a Zeta meter (ZM-77). The zeta potentials (PZ) were calculated with the Helmholtz–Smoluchowski equation [23].

2.3.3. Zero point charge (ZPC)

The ZPC was determined by the equation

$$\mathrm{ZPC_c} = \sum (\mathrm{IEP})_i X_i, \tag{2.1}$$

where X_i is the molar fraction and IEP_i is the isoelectric point of each component.

2.4. Surface complexation modeling

The surface complexation models used in this study were the constant capacitance model [13] and the triple layer model, modified to allow only inner-sphere complexes and both inner- and outer-sphere adsorption mechanisms, respectively [24]. Chemical assumptions, chemical reactions, intrinsic conditional equilibrium constants for protonation–dissociation and background electrolyte complex formation, and mass balance and charge balance equations used in the constant capacitance model and the triple layer model are discussed in detail in Goldberg [25].

Two methodologies were used to determine surface complexation constant values: (i) the double extrapolation technique [25,26], and (ii) optimization using the FITEQL 3.2 program [27].

For the AlSi and AlSiFe synthesized in this study, the ionic constants and capacitances were obtained with both the CCM and TLM using the software FITEQL 3.2. However, only the acidity constants for AlSiFe using the TLM were obtained by the double extrapolation technique. The FITEQL 3.2 software uses a nonlinear least-squares optimization technique to fit equilibrium constants to experimental potentiometric titration data. For each convergent optimization, FITEQL 3.2 provides the quality of fit criterion for a set of surface constants. This criterion, V_y, which is the weighted sum of squares of residues (SOS) divided by the degrees of freedom (DF), may be calculated using the equation [27]:

$$V_y = \frac{\mathrm{SOS}}{\mathrm{DF}} = \frac{\sum (Y_j/S_j)^2}{N_\mathrm{p} N_\mathrm{c} - N_\mathrm{u}}, \tag{2.2}$$

where Y_j is the mass residual balance calculated from the deviation between the calculated and experimental mass balance for the component j; S_j is the error calculated for Y_j from the experimental error estimates; N_p is the number of data points; N_c is the number of components for which both the total and the free concentrations are known; and N_u is the number of adjustable parameters. The value of V_y thus depends on the experimental error estimates, and higher error estimates produce lower values of V_y. In general, for a given set of error estimates, lower values of V_y indicate better fit between the experimental data and the model.

3. Results and discussion

3.1. Physicochemical characterization of synthetic aluminosilicate compounds

Transmission electron microscopy, Mösbauer spectroscopy, infrared spectroscopy, X-ray diffraction, and thermogravimetric analysis indicated that the synthetic aluminosilicate compounds, AlSi and AlSiFe, presented properties similar to those of natural allophanic compounds of andisols.

The transmission electron micrograph of AlSi (Fig. 1) shows spherical particles, which resemble those of natural allophanes [28]. The diameter of the AlSi particles varies from 10 to 30 nm, which is larger than that normally reported for the natural allophane (5–10 nm; [6]), but they do coincide in morphology with one allophanic sample from a Chilean andisol reported by Mora et al. [19]. However, Mora et al. [19] reported that the TEM image of clay minerals of the Chilean soils showed the formation of microaggregates not found in the TEM image of aluminosilicates.

The spectrum XRD (Fig. 2) of both aluminosilicates, AlSi and AlSiFe, present the characteristics of an amorphous material. This is consistent with the characteristics of allophanes, because they are usually referred to as an amorphous material to the X-rays and show a weak sign in the X-ray diffraction pattern [7].

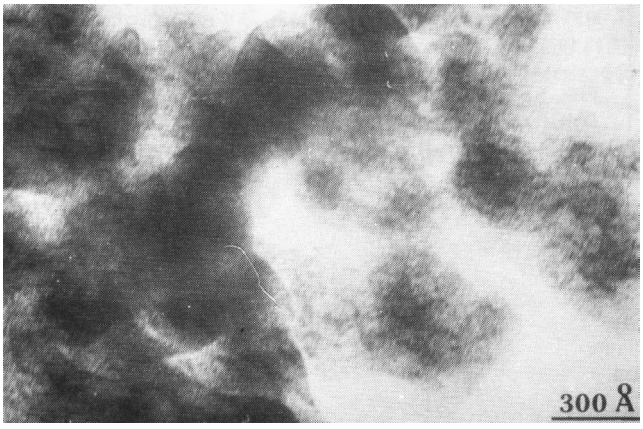

Fig. 1. Transmission electron microscopy microphotograph of noncrystalline aluminosilicate (AlSi).

The TGA indicates that both aluminosilicates are highly stable in the temperature range of the analysis, as observed in Figs. 3a (AlSi) and 3b (AlSiFe). The gradual variation of weight loss of both compounds as the temperature increases is due to dehydration of water molecules adsorbed on the surface observed at approximately between 90–100 °C, characteristic of amorphous compounds. The thermograms of crystalline compounds differ from those of amorphous compounds in that it is possible to differentiate the water retained by humidity and crystallization.

The ^{57}Fe Mössbauer spectra at 300 K of the AlSiFe show a paramagnetic doublet (Fig. 4). Such spectral behavior is caused by the superparamagnetism induced by the isomorphic exchange of aluminum for iron. This has been reported by Mora [29] using a chemical speciation program, GEOCHEM. Aluminum is conserved as Al^{3+} in the pH range of the synthesis, which implies that the Fe deposit on the AlSi surface is in the presence of Al^{3+}, which can produce an isomorphic exchange of Al for Fe. This process usually occurs in soils because the solubilization of allophane is particularly high at pH 3 with a high liberation of Al^{3+}.

The Mössbauer parameters, quadrupole splitting of doublet (Δ), linewidth (τ), and isomer shift (δ), were 0.85, 0.51, and 0.36 mm s^{-1}, respectively, which are typical values of Fe^{3+} high-spin oxyhydroxides (Fig. 4). The Fe^{3+} is octahedrally coordinated, which corresponds to a ferrihydrite type oxide, according to experimental evidence presented by Musić et al. in studies of oxide phases precipitated from concentrated $Fe(NO_3)_3$ solutions [30]. These results were previously discussed by Mora et al. [21] in the analysis of an aluminosilicate coated with iron oxide (AlSiFe).

FTIR spectra of the AlSi compounds are characterized by bands typical of allophane (Fig. 5), having a maximum transmittance at 3400 cm^{-1} from the stretching vibration of O–H and a transmittance at 1050 cm^{-1} from the stretching vibration of Si–O–Al [30]. The spectrum of AlSi shows a slight shift of bands when coated with iron oxide (AlSiFe), and the spectrum of AlSiFe shows the appearance of a new band at 1200 cm^{-1} presenting shift characteristic bands of iron oxides around 800–900 cm^{-1} [30]. The difference between the AlSiFe band and the iron oxide bands could be the result of the formation of covalent bonds between the Si–O–Fe and Al–O–Fe. During the synthesis of AlSiFe, the Fe deposited on the AlSi surface forms covalent bonds between the SiO^- groups and $Fe(OH)_2^+$, $FeOH^{2+}$, and Fe^{3+} species in solution due to the generation of electrostatic attractions.

3.2. The surface composition

The surface composition is not coincident with the bulk composition. Thus, it is possible to use the ZPC determined by the electrophoretic migration (IEP) to describe the surface charge. Gil-Llambías and Escudey-Castro [31] found that through the relationship between the IEP and the ZPC

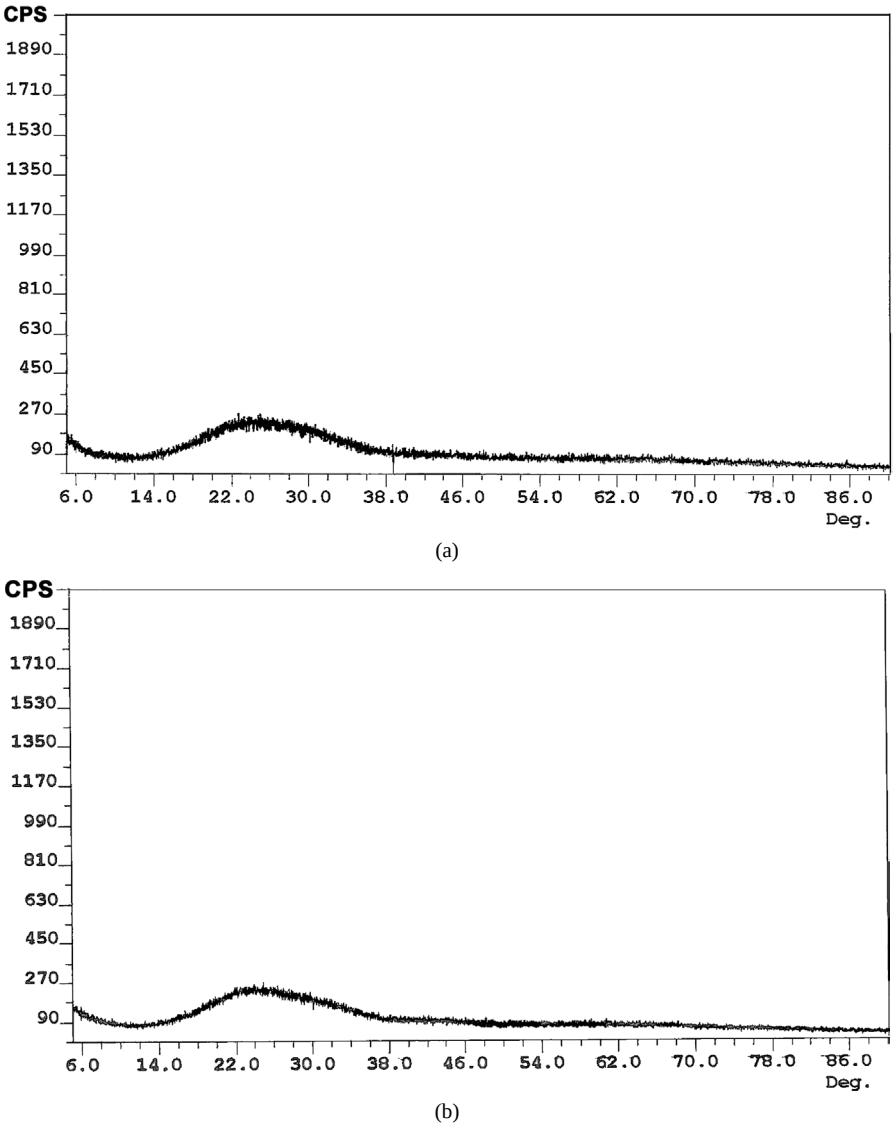

Fig. 2. X-ray diffractometry (XRD) of (a) aluminosilicate (AlSi) and (b) aluminosilicate coated with iron oxide (AlSiFe).

calculated using the Parks model (ZPC_c, [32]) it is possible to determine the surface composition.

From Eq. (2.1), it is then possible to determine the ZPC_c of the AlSi from both the bulk composition of AlSi and the IEP values of aluminum and silicon oxides (Table 1). The bulk composition of AlSi is 29% of aluminum oxide as Al_2O_3 and 71% of silicon oxide as SiO_2. Therefore, the ZPC_c value (4.1) is slightly lower than the IEP experimental value (4.47). These results demonstrate that exist SiOH and AlOH sites on the AlSi surface, with an important predominance of the SiOH sites (Table 2). The AlSi IEP (4.47) is a value ranging between the Al-oxide (8.3–9.4, Table 1) and Si-oxide (1.5–3.5, Table 1) IEP values.

For pure oxides the ZPC coincides with the IEP, because the charge generated in the *d*-plane of the diffuse layer is qualitatively represented on the surface composition of the solid [29]. The differences between the ZPC_c and IEP show a slight increase of AlOH sites with respect to the Al_2O_3 present in the bulk composition (34% Al_2O_3 on the surface; Table 2). This slight increase probably resulted from a sheet of aluminum hydroxide upon one side of which was a layer of silanol groups and later reaction with an excess of $Si(OH)_4$. In these reactions may take place an isomorphic exchange of aluminum for silicon [33] that generates a structural negative charge, then the IEP decrease.

When the aluminosilicate is coated with iron oxide (AlSiFe), the ZPC_c (4.4) is lower than the IEP (8.46), which shows that there is not coincidence of the bulk composition (Table 2). It demonstrates that the surface composition was formed mainly for iron oxide. Mora et al. [19] showed that when the AlSiFe was recovered with 12% of iron oxide, with the IEP (8.6, Table 1) not changed, then through the IEP value it was demonstrated that the surface of AlSi was completely covered in the first step for iron oxide and later, this oxide continued being developed with a second coverage with the same characteristics.

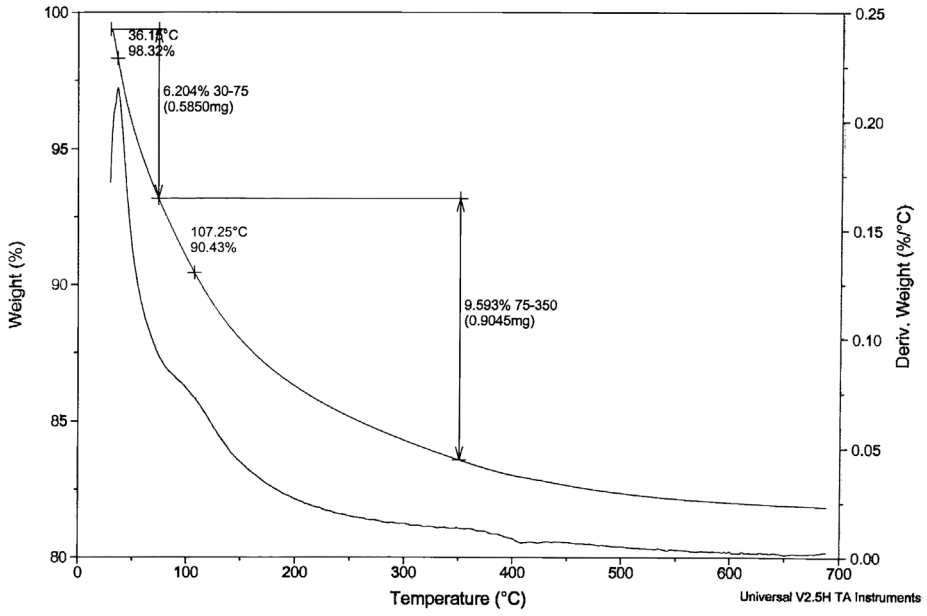

(a)

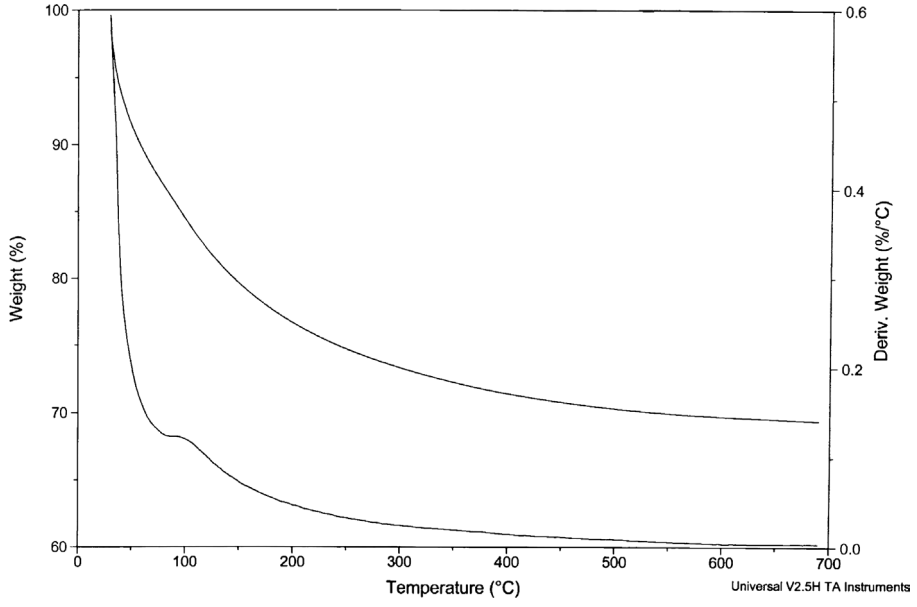

(b)

Fig. 3. Thermogravimetric analysis (TGA) of (a) aluminosilicate (AlSi) and (b) aluminosilicate coated with iron oxide (AlSiFe).

The IEP value (8.46) increased considerably with respect to the AlSi IEP value (4.47). The results are evidence of the change of the active sites of the external surface mainly correspond to FeOH sites. Then, the coverage surface of AlSiFe is homogeneous, while the internal surface remains heterogeneous.

3.3. Surface complexation modeling

The point of zero salt effect (PZSE) was also characterized in order to improve the understanding of the physicochemical and mineralogical processes that control the clay dispersion and the colloidal properties of the resulting suspensions. The PZSE value for AlSi is 6.2. There is a shift in PZSE toward a low pH when the aluminosilicate is coated with iron oxide ($PZSE_{AlSiFe}$ 4.8). If these results are compared with other values reported (Table 1), it is possible to observe that the PZSE of Al-oxides (8.5) > Fe-oxides (7.9) > AlSi (6.2) > AlSiFe (4.8) > Si-oxides (2.9) [8]. The decrease of PZSE can be explained by the different types of hydroxyl groups on the oxide surfaces. These types of groups have different reactivities, depending upon the coordination environment of the oxygen in the FeOH, AlOH, and SiOH groups [34].

As discussed above, the surface reactivity is modified by the displacement of electronic density in the metal on the ex-

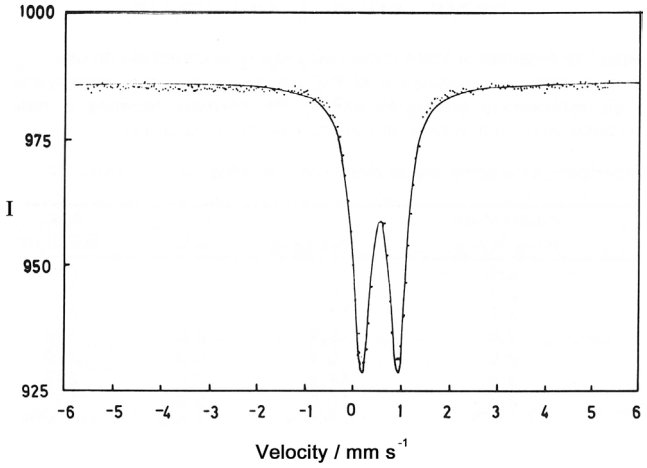

Fig. 4. Mössbauer spectrum of aluminosilicate coated with iron oxide (AlSiFe), recorded at 300 K.

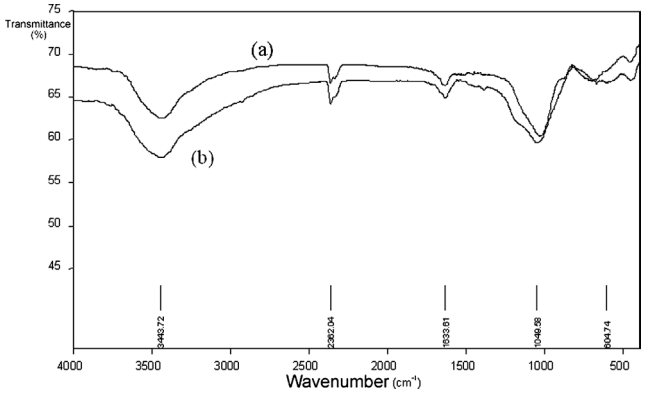

Fig. 5. FTIR spectra of aluminosilicate (AlSi) and aluminosilicate coated with iron oxide (AlSiFe), recorded at room temperature.

Table 1
Comparison of points of zero charges for several solid phases in suspension

Solid	PZSE[a]	IEP[a]	ZPC[c]
AlSi	6.2	4.47	4.1
AlSiFe	4.8	8.46	4.4
AlSiFe-II (12% Fe_2O_3)	5.2[b]	8.6[b]	3.9[b]
Alon (γ-Al_2O_3)	8.5[c]	8.3–9.4[d]	–
Ferrihidrite (FeO(OH))	7.9[e]	–	–
Goethite (α-FeOOH)	7.3[c]	6.4–8.7[d]	–
Kaolinite ($Si_4Al_4O_{10}(OH)_8$)	4.5–5.0[c]	–	–
Quartz (α-SiO_2)	2.9[c]	1.5–3.5[d]	–

[a] Experimental values.
[b] Ref. [19].
[c] Averages [8].
[d] Ranges of IEP using (Na, K) Cl, NO_3, ClO_4, as background electrolyte [46].
[e] Ref. [43].

ternal layer. For example, when the Fe atoms bonded with the Si–O the acidity of the active sites of the surface increased [19]. Therefore, the surface becomes more negative as pH increases (Fig. 6).

The ZPC measured by electrophoretic mobility (IEP) only describes the external surface of the oxides (corresponding to the shear-plane, located between the *o*-plane and *d*-plane) [31]; meanwhile the ZPC determined by potentiometric titration (PZSE) consider the internal and external sites. Therefore, only these parameters are coincident when the solid is pure oxide. Thus, if the heterogeneous surfaces are compared using both IEP and PZSE values, they show different behavior of the surface [29].

Table 2
Physicochemical properties of allophanic synthetic compounds: aluminosilicate (AlSi) and aluminosilicate coated with iron oxide (AlSiFe)

Solid	SiO_2/Al_2O_3	Iron oxide (Fe_2O_3) (%)	Al_2O_3 (%)	SiO_2 (%)	Fe_2O_3 (%)	SSA[a] ($m^2\ g^{-1}$)
AlSi	2.4	–	29[b] 34[c]	71[b] 66[c]	–	674
AlSiFe	2.2	5.0	31.8[b]	66.7[b]	1.5[b]	341

[a] Specific surface area.
[b] Bulk composition of the sample.
[c] Composition of AlSi external surface, determined using experimental IEP value.

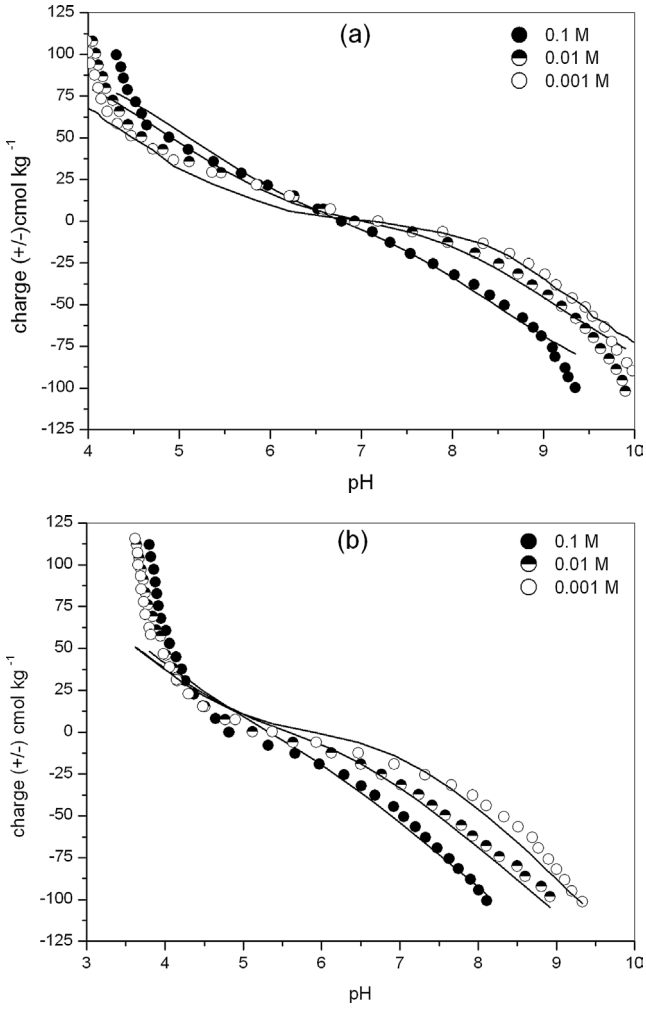

Fig. 6. Potentiometric titrations of (a) aluminosilicate (AlSi) and (b) aluminosilicate coated with iron oxide (AlSiFe) fitted with the constant capacitance model.

Table 3
Description of experimental parameters used in the application of the constant capacitance model on synthetic allophanic compounds

Parameter	Value	
	AlSi	AlSiFe
Surface area ($m^2\ g^{-1}$)	674	341
Site density (sites nm^{-2})	0.98	3.00
Inner-layer capacitance ($F\ m^{-2}$)	2.0	3.0
Suspension density ($g\ L^{-1}$)	3.0	3.0

Table 4
Description of the experimental parameters used in the application of the triple layer model on synthetic allophanic compounds

Parameter	Value	
	AlSi	AlSiFe
Surface area ($m^2\ g^{-1}$)	674	341
Site density (sites nm^{-2})	0.98	3.00
Inner-layer capacitance ($F\ m^{-2}$)	2.2	3.0
Outer-layer capacitance ($F\ m^{-2}$)	0.2	0.2
Suspension density ($g\ L^{-1}$)	3.0	3.0

Table 5
Numerical values of intrinsic surface complexation constants as a function of ionic strength using the constant capacitance model

	I (M)	$pK_{a_1}^{int}$	$pK_{a_2}^{int}$	SOS/DF	c ($F\ m^{-2}$)
AlSi	10^{-1}	5.65	7.92	94	2.0
(Ns = 0.98	10^{-2}	5.45	8.59	155	2.0
sites nm^{-2})	10^{-3}	5.15	8.62	927	3.0
AlSiFe	10^{-1}	4.15	6.50	560	3.0
(Ns = 3.00	10^{-2}	4.03	7.12	457	3.0
sites nm^{-2})	10^{-3}	3.61	8.14	514	3.0

In order to provide a correct chemical representation of a surface structure, independent experimental evidence must be used to choose the appropriate chemical surface complexation model. The surface complexation models used for the synthetic allophanic compounds were the constant capacitance model (CCM), previously reported by Mora [29] at ionic strength 0.1 M, and the triple layer model (TLM). The constant parameters were (i) surface site density, whose value was determined experimentally by maximum anion adsorption, and (ii) inner layer capacitance (c_1), an adjustable parameter in the TLM (Tables 3 and 4).

The equilibrium constants for the protonation and dissociation reactions were obtained with the CCM by the FITEQL 3.2 program and showed the surface charge difference in both aluminosilicates (AlSi and AlSiFe, Table 5). The presence of iron oxides on the surfaces of AlSi caused an increase in the surface acidity, leading to a change in the magnitude of the constant values.

The CCM was used to fit the acidity constant values to the potentiometric titrations at each ionic strength (Table 5), although this model is applicable in theory only to systems at high ionic strength [8]. The evaluation of potentiometric titrations was done separately because the FITEQL 3.2 program was not able to fit them simultaneously (Fig. 6), and $pK_{a_1}^{int}$ and $pK_{a_2}^{int}$ values are only valid for a particular ionic strength [14,35].

Table 6
Numerical values of intrinsic surface complexation constants using the constant capacitance model and triple layer model

Solid	$pK_{a_1}^{int}$	$pK_{a_2}^{int}$	$pK_{a_{X-}}$	$pK_{a_{M+}}$	Capacitance ($F\ m^{-2}$)
Constant capacitance model (CCM)					
AlOOH[a]	7.38	9.09	–	–	1.06
α-FeOOH[b]	7.31	8.80	–	–	1.06
FeOOH[c]	6.7	9.6	–	–	3.2
AlSi[d]	5.6	7.9	–	–	1.06
AlSiFe[d]	4.1	6.5	–	–	2.0
Triple layer model (TLM)					
SiO_2[e]	2.0	7.2	–	6.7	$c_1 = 1.4$, $c_2 = 0.2$
AlOOH[a]	5.0	11.2	7.5	8.6	$c_1 = 1.2$, $c_2 = 0.2$
α-FeOOH[b]	4.3	9.8	5.4	9.3	$c_1 = 1.2$, $c_2 = 0.2$
FeOOH[c]	4.8	10.8	8.6	7.7	$c_1 = 1.5$, $c_2 = 0.2$
AlSi[d]	6.02	8.13	6.77	6.98	$c_1 = 1.2$, $c_2 = 0.2$
AlSiFe[d]	3.46	7.16	5.12	5.58	$c_1 = 3.0$, $c_2 = 0.2$

[a] Averages of γ-Al_2O_3, 0.1 M NaCl as background electrolyte [40,41].
[b] Averages of goethite, 0.1 M NaCl as background electrolyte [44].
[c] Amorphous iron oxide, 0.1 M KCl as background electrolyte [42,43].
[d] Aluminosilicates, 0.1 M KCl as background electrolyte.
[e] 7×10^{-3} M NaCl as background electrolyte [45].

The results in Table 5 show that as ionic strength changes a low variation in $pK_{a_1}^{int}$ and $pK_{a_2}^{int}$ can be observed. The capacitance value was considered constant at all ionic strength, assuming the conditional character of the CCM with respect to the ionic strength that avoids the quantification of electrolyte binding [35]. When the ionic strength increases, the affinity for H^+ on the surface increases [36]. Thus, there is an increase in the $pK_{a_1}^{int}$ value because the surface acidity decreases. When the ionic strength decreases, the affinity for H^+ decreases and the affinity for OH^- increases, corresponding to an increase in $pK_{a_2}^{int}$ value.

According to Barrow [37], an increase in the $pK_{a_1}^{int}$ is expected, due to an increase in ionic strength that produces a decrease in the surface adsorption potential. In this model, the counterion balance is located in either the outer Helmholtz layer or the diffuse layer [38]. Therefore, if the surface is negatively charged, it becomes less negatively charged, and vice versa. For AlSi, the $pK_{a_1}^{int}$ (5.65) determined by the CCM is below the PZSE (6.2). Therefore, an increase in the ionic strength causes the surface to become less positive, favoring adsorption of protons and thus shifting the $pK_{a_1}^{int}$ toward higher pH values.

If we compare the values obtained for acidity constants of synthetic aluminosilicates with acidity constant of pure oxides reported in the literature using CCM (Table 6), it is possible to observe the differences among the surfaces of Al oxides, Fe oxides, Si oxides, AlSi, and AlSiFe. These differences result from (i) the acidity of metal constituent of the surface sites (AlOH, FeOH, SiOH): the pure oxides have the same internal and external groups, but synthetic aluminosilicates do not present the same reactivity on the

internal and external groups; (ii) the fit of intrinsic acidity constants: these values are dependent on the capacitance and surface site density values; (iii) the presence of silicon in the synthetic aluminosilicates: the surface SiOH sites produce a decrease in $pK_{a_1}^{int}$ and $pK_{a_2}^{int}$ values. This change is attributed to the fact that the Si atom is more acidic than Al and Fe atoms (ratio charge/radius Si = 0.154, Al = 0.053, and Fe = 0.037); therefore the reactivity of Fe and Al atoms is modified when Si–O–Fe or Si–O–Al are bonded.

When both aluminosilicates are compared at ionic strength 0.1 M, the coating with iron oxide on the AlSi surface causes the $pK_{a_s}^{int}$ values to be more acidic ($pK_{a_1}^{int} = 4.15$, $pK_{a_2}^{int} = 6.50$) than $pK_{a_s}^{int}$ values of AlSi ($pK_{a_1}^{int} = 5.65$, $pK_{a_2}^{int} = 7.92$). The difference between the $pK_{a_s}^{int}$ values is primarily attributed to the modification of surface site reactivity by the silicon presence in the internal surface (Si–O–Al and Si–O–Fe). The most important reason for the increase in acidity of AlSiFe is the acidity difference of the external FeOH groups and the FeOH groups present at the AlSi/Fe-oxide interface, due to the chemical reaction that occurs during the formation of the first layers of Fe-oxides on AlSi when the $SiOH_{(s)}$ surface reacts with $[Fe(OH)(H_2O)_5]^{2+}$ and $[Fe(OH)_2(H_2O)_4]^{+}$ species in solution. The formation of Si–O–Fe bonds modifies the reactivity of oxygen of the water molecules that are coordinated by chemisorption to the Fe atoms [29,38].

The CCM contains a limited number of variables, making it a simple model for the interpretation of surface reactivity. However, the model is restricted to describing ion adsorption via inner sphere surface complexes. Therefore, to describe the outer sphere complex, it was necessary to use the TLM, where the number of adjustable parameters is greater than for the CCM [25].

The acidity constants obtained by the CCM were used in the input of the FITEQL 3.2 program to estimate the acidity and complexation surface constants by the TLM for both aluminosilicates (AlSi and AlSiFe). For AlSiFe, the acidity constants were obtained using the double-extrapolation procedure [26], since the FITEQL 3.2 program showed an incapacity to discriminate between the protonation and dissociation constants, which resulted in values not chemically possible ($pK_{a_1}^{int} > pK_{a_2}^{int}$). The inner capacitance and surface complexation constants values were fit later using FITEQL 3.2 program (Fig. 7b).

When the complexation constants for AlSiFe were compared (Table 7) at the same ionic strength, 0.1 M, it can be seen that they are very close ($pK_{Cl^-}^{int} = 5.11$ and $pK_{K^+}^{int} = 5.58$). With the same $pK_{a_s}^{int}$ values at decreased ionic strength, 0.01 M, these values were very similar to the previous: $pK_{Cl^-}^{int} = 5.91$ and $pK_{K^+}^{int} = 5.17$. Therefore, the pK_c^{int} values are relatively constant in the range of ionic strengths studied. The reactions of the surface with the background electrolyte are charge-balanced on each side of the electric double layer/solution. Thus, terms of equal magnitude ($pK_{Cl^-}^{int} \approx pK_{K^+}^{int}$) determined by the same concentration

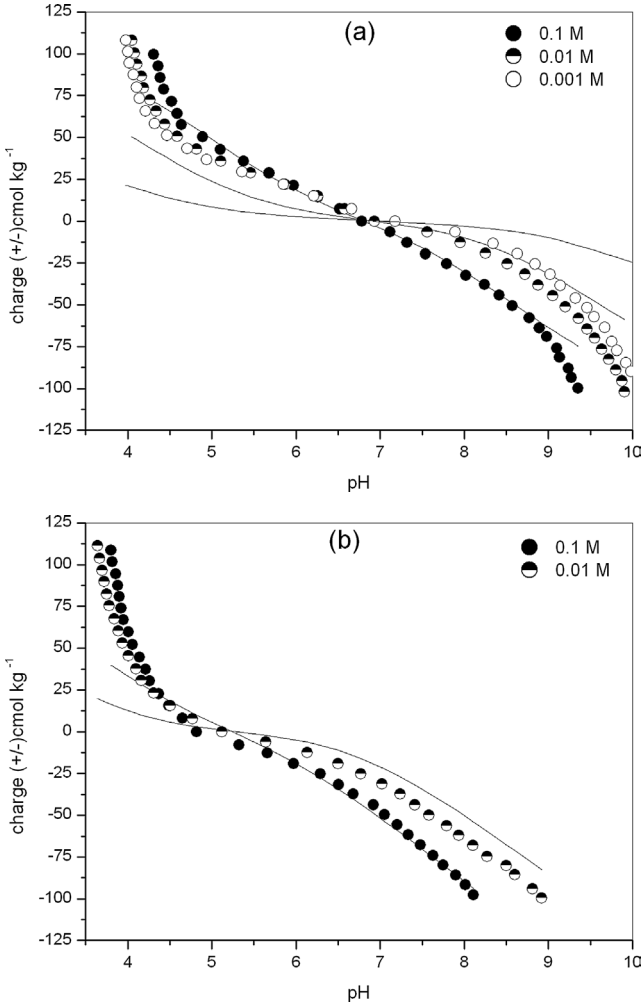

Fig. 7. Potentiometric titrations of (a) aluminosilicate (AlSi) and (b) aluminosilicate coated with iron oxide (AlSiFe) fitted with the triple layer model, using constant values obtained at ionic strength 0.1 M (KCl).

Table 7
Numerical values of intrinsic surface complexation constants as a function of ionic strength of AlSiFe using the triple layer model

	I (M)	$pK_{a_1}^{int}$	$pK_{a_2}^{int}$	$pK_{a_{Cl^-}}$	$pK_{a_{K^+}}$	SOS/DF	c_1 (F m^{-2})
AlSiFe	10^{-1}	3.46[a]	7.16[a]	5.12[b]	5.58[b]	305	3.1
Ns = 3.00	10^{-2}	3.46[a]	7.16[a]	5.91[b]	5.17[b]	222	3.4
sites nm^{-2}	10^{-3}	3.46[a]	7.16[a]		No convergence		

[a] Values obtained by the double extrapolation technique.
[b] Values fitted with FITEQL 3.2.

of counterions (Cl^- and K^+) from the solution ensure mass balance on the solution side of the interface [39].

On the other hand, it was possible to fit simultaneously the acidity constant values for AlSi (Fig. 7a). When the ionic strength decreased only scarce variations of $pK_{a_1}^{int}$ and $pK_{a_2}^{int}$ values were observed. However, the $pK_{Cl^-}^{int}$ values increased, while the $pK_{K^+}^{int}$ values decreased (Table 8). Then, if the ionic strength decreased the positive values became less positive

Table 8
Numerical values of intrinsic surface complexation constants as a function of ionic strength of AlSi using the triple layer model (FITEQL 3.2 program)

	I (M)	$pK_{a_1}^{int}$	$pK_{a_2}^{int}$	pK_{Cl^-}	pK_{K^+}	SOS/DF
AlSi	10^{-1}	6.02	8.13	6.77	6.98	82
Ns = 0.98	10^{-2}	6.26	8.11	7.52	6.61	145
sites nm^{-2}	10^{-3}	6.78	8.05	9.05	5.38	1153

and negative values less negative of the surface charge and the ions of background electrolyte are dispersed near the surface [37]. Therefore, the distance between the superficial *o*-plane and the *d*-plane increases.

The increase of ionic strength increases the concentration of counterions close to the surface, which produces changes in the electric potential as ions are distributed from the surface to the solution. These changes increase the affinity of ions for the surface; therefore the $pK_{Cl^-}^{int}$ and $pK_{K^+}^{int}$ values obtained are expected [37].

According to Guerin and Reaman [39], at lower ionic strengths the distribution of counter ions in the electric double layer was from the *o*-plane to the solution. So it was necessary to consider a factor of correction derived from the electric double layer theory to account for the effects of surface charge. The results obtained showed a better approximation of the charge distribution, and therefore at low ionic strength the pK_c^{int} values could be overestimated with respect to the ionic strength 0.1 M.

The results obtained for AlSi and AlSiFe by the TLM were in agreement with the results obtained using the CCM. However, the CCM and the TLM only showed a good description from pH 4.5 to 8.5. Thus, at pH below 4.5 and above 8.5 the parameters determined are not able to describe the systems studied, mainly due to the dissolution of the mineral component in these extreme pH values [19].

On the other hand, the parameters obtained using the CCM ($pK_{a_1}^{int}$, $pK_{a_2}^{int}$, and capacitance values) and the TLM ($pK_{a_1}^{int}$, $pK_{a_2}^{int}$, $pK_{Cl^-}^{int}$, $pK_{K^+}^{int}$, and inner capacitance) showed that the surface behavior of the synthetic aluminosilicates is different from that of the pure oxides, such as Al oxide [40,41], Fe oxide [42–44], and Si-oxide [45] surfaces, since these present homogeneous surfaces (Table 6).

The acidity constants obtained using CCM and TLM do not present important differences. However, the TLM describes the background electrolyte behavior while the CCM does not consider the asymmetry of the charge distribution. Then, the acidity and complexation constants determined by TLM are more approximate values to real systems.

4. Conclusion

The synthetic aluminosilicates showed structural characteristics similar to natural allophanes and iron oxide amorphous.

The ZPC calculated by the Parks model (ZPC_c) compared with IEP values showed that on the aluminosilicate surface was slightly enriched by AlOH. For aluminosilicate coated with iron oxide the ZPC_c was lower than IEP showing that the surface composition is formed mainly for iron oxide.

Both the constant capacitance model (CCM) and the triple layer model (TLM) were able to describe the surface behavior of both synthetic aluminosilicates. However, better fits were obtained to higher ionic strengths.

The change of ionic strength showed a good relation with the parameters obtained using the CCM and the TLM. However, the TLM better described the surface charge distribution when the ionic strength changed. Then, the acidity and complexation constants determined by TLM are more approximate values to real systems.

Acknowledgment

We acknowledge the support of FONDECYT Grant 2000110.

References

[1] T. Henmi, K. Wada, Am. Mineral. 61 (1976) 379.
[2] S.I. Wada, K. Wada, Clay Miner. Bull. 12 (1977) 289.
[3] J.N.R. Ryan, M. Elimelech, Colloids Surf. A Physicochem. Eng. Aspects 107 (1996) 1.
[4] R.L. Parfitt, Aust. J. Soil Res. 28 (1990) 343.
[5] E. Besoain, in: J. Tosso (Ed.), Instituto de Investigaciones Agropecuarias, Ministerio de Agricultura, Santiago Press, 1985, p. 109.
[6] K. Wada, in: J.B. Dixon, S.B. Weed (Eds.), Minerals in Soil Environments, second ed., Soil Science Society of America, Madison, WI, 1989.
[7] J.P. Gustafsson, E. Karltun, P. Bhattacharya, Research Report TRITA-AMI 3046, 1998.
[8] G. Sposito, The Surface Chemistry of Soils, Oxford Univ. Press, New York, 1984.
[9] D.A. Dzombak, F.M.M. Morel, Surface Complexation Modeling: Hydrous Ferric Oxide, Wiley, New York, 1990.
[10] Y. Arai, D.L. Sparks, J. Colloid Interface Sci. 241 (2001) 317.
[11] M. Grafe, M.J. Eick, P.R. Grossl, A.M. Saunders, J. Environ. Quality 31 (2002) 1115.
[12] J.A. Dyer, P. Trivedi, N.C. Scivner, D.L. Sparks, J. Colloid Interface Sci. 270 (2004) 56.
[13] W. Stumm, R. Kummert, L. Sigg, Croat. Chem. Acta 53 (1980) 291.
[14] J.A. Davis, R.O. James, J.O. Leckie, J. Colloid Interface Sci. 63 (1978) 480.
[15] J.A. Davis, J.O. Leckie, J. Colloid Interface Sci. 67 (1980) 90.
[16] J.A. Davis, J.O. Leckie, J. Colloid Interface Sci. 74 (1980) 32.
[17] G. Sposito, J. Colloid Interface Sci. 91 (1983) 329.
[18] P. Díaz, G. Galindo, M. Escudey, Bol. Soc. Chil. Quim. 35 (1990) 381.
[19] M.L. Mora, M. Escudey, G.G. Galindo, Bol. Soc. Chil. Quim. 39 (1994) 237.
[20] B. Bernas, Anal. Chem. 40 (1968) 1682.
[21] M.L. Mora, C.M. Escudey, G.G. Galindo, in: E. Baggio-Saitovitch, E. Galvao da Silva, H.R. Rechemberg (Eds.), Applications of the Mössbauer Effect, World Scientific, London, 1990, p. 419.
[22] M.D. Heilman, D.L. Carter, C.L. González, Soil Sci. 100 (1965) 409.
[23] K.J. Hunter, Zeta Potential in Colloid Science: Principles and Applications, Academic Press, London, 1981.

[24] K.F. Hayes, J.O. Leckie, ACS Symp. Ser. 323 (1986) 114.
[25] S. Goldberg, Adv. Agron. 42 (1992) 233.
[26] R.O. James, J.A. Davis, J.O. Leckie, J. Colloid Interface Sci. 65 (1978) 331.
[27] A.L. Herbelin, J.C. Westall, Report 96-01, Dept. of Chemistry, Oregon State University, Corvallis, 1996.
[28] R.L. Parfitt, Adv. Agron. 30 (1978) 1.
[29] M. Mora, Ph.D. thesis, Universidad de Santiago de Chile, 1992.
[30] S. Musić, G.P. Santana, G. Šmit, V.K. Garg, Croat. Chem. Acta 72 (1999) 87.
[31] F.J. Gil-Llambías, A.M. Escudey-Castro, J. Chem. Soc. Chem. Commun. (1982) 478.
[32] G.A. Parks, Adv. Chem. Ser. 67 (1967) 121.
[33] F.J. Doucet, C. Schneider, S.J. Bones, A. Kretchmer, I. Moss, P. Tekely, C. Exley, Geochim. Cosmochim Acta 65 (2001) 2461.
[34] J.A. Davis, D.B. Kent, Rev. Mineral. Geochem. 23 (1990) 177.
[35] J. Lützenkirchen, J. Colloid Interface Sci. 217 (1999) 8.
[36] R.J. Atkinson, A.M. Posner, J.P. Quirk, J. Phys. Chem. 71 (1967) 550.
[37] N.J. Barrow, Austr. J. Soil Res. 37 (1999) 787.
[38] F.J. Hingston, A.M. Posner, J.P. Quirk, J. Soil Sci. 23 (1972) 177.
[39] M. Guerin, J.C. Reaman, J. Colloid Interface Sci. 250 (2002) 492.
[40] R. Sprycha, J. Colloid Interface Sci. 127 (1989) 1.
[41] R. Sprycha, J. Colloid Interface Sci. 127 (1989) 12.
[42] M. Escudey, M. Mora, I. Salazar, G. Galindo, Bol. Soc. Chil. Quim. 32 (1987) 199.
[43] M. Escudey, P. Díaz, G. Galindo, Contribuciones Cient. Tec. 78 (1987) 23.
[44] P. Zhang, D.L. Sparks, Environ. Sci. Technol. 24 (1990) 1848.
[45] T.N.T. Phan, N. Louvard, S.-A. Bachiri, J. Persello, A. Foissy, Colloids Surf. A Physicochem. Eng. Aspects 244 (2004) 131.
[46] D.G. Kinniburgh, M.L. Jackson, in: M.A. Anderson, A.J. Rubin (Eds.), Adsorption of Inorganics at Solid–Liquid Interfaces, Ann Arbor Science Pub., Ann Arbor, 1981, pp. 91–160.